Biogeosciences Discuss., 12, 15901–15924, 2015
www.biogeosciences-discuss.net/12/15901/2015/
doi:10.5194/bgd-12-15901-2015

Biogeosciences Discussions
Open Access

Improving estimations of greenhouse gas transfer velocities by atmosphere–ocean couplers in Earth-System and regional models

V. M. N. C. S. Vieira[1], E. Sahlée[2], P. Jurus[3,6], E. Clementi[4], H. Pettersson[5], and M. Mateus[1]

[1]MARETEC, Instituto Superior Técnico, Universidade Técnica de Lisboa, Av. Rovisco Pais, 1049-001, Lisboa, Portugal
[2]Dept. of Earth Sciences, Air Water and Landscape sciences, Villavägen 16, 75236 Uppsala, Sweden
[3]DataCastor, Prague, Czech Republic
[4]Istituto Nazionale di Geofisica e Vulcanologia, INGV, Bologna, Italy
[5]Finnish Meteorological Institute, P.O. Box 503, 00101 Helsinki, Finland
[6]Institute of Computer Science, Czech Academy of Sciences, Czech Republic

Received: 1 August 2015 – Accepted: 3 September 2015 – Published: 28 September 2015

Correspondence to: V. M. N. C. S. Vieira (vasco.vieira@tecnico.ulisboa.pt)

Published by Copernicus Publications on behalf of the European Geosciences Union.

Abstract

Earth-System and regional models, forecasting climate change and its impacts, simulate atmosphere–ocean gas exchanges using classical yet too simple generalizations relying on wind speed as the sole mediator while neglecting factors as sea-surface agitation, atmospheric stability, current drag with the bottom, rain and surfactants. These were proved fundamental for accurate estimates, particularly in the coastal ocean, where a significant part of the atmosphere–ocean greenhouse gas exchanges occurs. We include several of these factors in a customizable algorithm proposed for the basis of novel couplers of the atmospheric and oceanographic model components. We tested performances with measured and simulated data from the European coastal ocean, having found our algorithm to forecast greenhouse gas exchanges largely different from the forecasted by the generalization currently in use. Our algorithm allows calculus vectorization and parallel processing, improving computational speed roughly 12× in a single cpu core, an essential feature for Earth-System models applications.

1 Introduction

The role of the oceans and seas as sinks or sources of greenhouse gases is highly variable in space and time, depending on the local biogeochemical cycles and air–water gas exchanges. This holds for CO_2 (Smith and Hollibaugh, 1993; Cole and Caraco, 2001; Takahashi et al., 2002, 2009; Inoue et al., 2003; Duarte and Prairie, 2005; Borges et al., 2005; Rutgersson et al., 2008; Lohrenz et al., 2010; Torres et al., 2011; Rödenbeck et al., 2013; Schuster et al., 2013; Landschützer et al., 2014; Arruda et al., 2015; Brown et al., 2015; Harley et al., 2015) for CH_4 (Harley et al., 2015) and for N_2O (Bange et al., 1996; Nevison et al., 1995, 2004; Walter et al., 2006; Barnes and Goddard, 2011; Sarmiento and Gruber, 2013; Harley et al., 2015). Regional and Earth-System Models (ESM), constrained by calculus demands and because the main driver of atmosphere–ocean gas transfers is turbulence due to wind friction over the

BGD
12, 15901–15924, 2015

sea-surface, have estimated gas transfer velocities from an older formulation by Wanninkohf (1992) considering the effect of wind speed 10 m above sea-surface (u_{10}) but disregarding the complexity of processes more recently unveiled. The Ocean Carbon-Cycle Model Intercomparison Project, during its Phase 2 (1998–2000), established Wanninkohf's formulation in its protocol (OCMIP, 2004). The Istituto Nazionale di Geofisica e Volcanologia (INGV) in cooperation with the Centro Euro–Mediterraneo sui Cambiamenti Climatici (CMCC) developed the INGV-CMCC's Carbon Cycle Earth-System Model (ICC-ESM: Fogli et al., 2009), estimating the atmosphere–ocean CO_2 flux by the marine biogeochemistry model PELAGOS (Vichi et al., 2007a, b). Used in the ENSEMBLES project funded by the 6th Framework Program for the prediction of climate change impacts at the seasonal, decadal and centennial timescales, it forecasts the Mediterranean, the equatorial Pacific and the Southern Ocean as sinks of anthropogenic CO_2 whereas the northern Atlantic, northern Pacific and Indic ocean shift towards net sources (Vichi et al., 2011). It is also being used in the MedSea project funded by the 7th Framework Program (FP7) for the prediction of sea acidification impacts under climate change scenarios. PELAGOS is a Global Ocean generalization of the Biogeochemical Flux Model (BFM) used in regional applications to estimate the Mediterranean primary production (Lazzari et al., 2012) and to access the wind-driven response of the Mediterranean biogeochemistry (Mattia et al., 2012). Despite efforts to keep these as state-of-the art, with BFM being currently under version 5 and PELAGOS being tested interacting with the Nucleus for European Modelling of the Ocean (NEMO) oceanographic modelling framework (Visinelli, 2014), both still estimate the air–water transfer velocity from Wanninkhof's formulation. The EPOCA project, funded by the European Commission under FP7, focused on the worldwide consequences of ocean acidification due to the increased concentrations of CO_2 in the biosphere. By coupling the Bern3D ocean circulation model with the PISCES biogeochemical model, it forecasts a decreased incorporation of $CaCO_3$ in planktonic shells and its feedback to atmospheric CO_2 (Gangsto et al., 2011). PISCES evolved from HAMOCC3.1 and HAMOCC5, also using Wanninkhof's formulation. Still within EPOCA's research, Artioli et al. (2012) coupled the POLCOMS 3-D ocean circulation model with the ERSEM ocean biogeochemical model to simulate the North Sea carbonate system, having found that uncertainty about pH and pCO_2 must be reduced. Wanninkhof's formulation was also used to estimate the atmosphere–ocean CO_2 exchange over the Atlantic and Artic (Schuster et al., 2013) and over the global ocean (Rodenbeck et al., 2013). The regional oceanographic numerical lab MOHID allows the user to choose between the air–water gas exchange formulations by Carini et al. (1996) and Raymond and Cole (2001), which only account for u_{10}, or by Borges et al. (2004), also accounting for current drag with the bottom. These are empirical formulations best fitting low wind data collected from estuaries and neglecting fundamental factors as sea surface agitation and atmospheric stability. Nevertheless, they were applied to Iberia's coastal ocean in an attempt to estimate its CO_2 dynamics (Oliveira et al., 2012).

Earth-System Models further justifies the use of Wanninkhof's formulation on the basis of being designed for estimates over wide time intervals. ICC-ESM runs on 1day iteration intervals, PISCES' implementation on 2 h intervals and HAMMOCC5 updated solubilities on a monthly basis. Furthermore, with cells roughly 1100 km wide, as was the case of EPOCA, any cell from the water compartment is basically dominated by the deep fetch unlimited open ocean. But although it comprises roughly 95 % of the world oceans, in the remaining coastal ocean occur a significant part of the atmosphere–ocean CO_2 transfers related to the terrestrial inputs of carbon (Smith and Hollibaugh, 1993; Cole and Caraco, 2001; Duarte and Prairie, 2005; Borges et al., 2005), about 14 to 30 % of the global marine primary production (Gattuso et al., 1998), and about 40 % of the organic carbon burial in the sediments (Muller-Karger et al., 2005). Therefore, the biogeoscience and climate change community is well aware of the necessity to model the planetary system with a finer resolution for space, time and processes. Hence, the European Commission's Horizon 2020 included a specific call for this subject.

We use the Weather Research and Forecasting Model (WRF) with the 2-way coupled wave–current modelling system WaveWatch III (WW3)–NEMO to test alternatives on how to couple atmospheric and oceanographic sub-models taking into account some

BGD
12, 15901–15924, 2015

of the so often neglected mediator processes. The transfer velocities estimated by Wanninkhof's formulation and the new alternatives are compared using the numerical schemes and software by Vieira et al. (2013), updated in the processes when required as described below, and in the calculus vectorization and parallel processing. The Matlab based software version 2.0 is available at http://www.maretec.org/en/publications/.

2 Methods

2.1 The field data for model validation

The competing formulations were tested with measurements by the atmospheric tower at the Östergarnsholm site in the Baltic Sea, located at 57°27′ N and 18°59′ E, the Submersible Autonomous Moored Instrument (SAMI-CO_2) 1 km away and the Directional Waverider 3.5 km away, both south-eastward (Rutgersson et al., 2008), performed from the 22 May 2014 at 12:00 LT to the 26 May 2014 at 00:00 LT. The CO_2 transfer velocities were estimated from $k_w = F/(C_a/k_H - C_w)$, were F was the air–water fluxes ($\mathrm{mol\,m^{-2}\,s^{-1}}$) measured by eddy-covariance (E-C), smoothed over 30 min bins and subject to the Webb–Pearman–Leuning (WPL) correction (Webb et al., 1980), C_a and C_w the measured air and water concentrations ($\mathrm{mol\,m^{-3}}$), and k_H the Henry constant (scalar) estimated for the measured temperatures, salinity and air pressure either from Weiss (1974) and Weiss and Price (1980) or form Johnson (2010) formulations. Were only used the data relative to when the wind direction set the SAMI sensor and Directional Waverider in the footprint of the atmospheric tower (90° < wind direction < 180°).

2.2 The simulated data to test the coupler

The competing formulations were tested with simulated data relative to the European shores from the 24 May 2014 at 06:00 LT to the 27 May 2014 at 00:00 LT. The atmospheric model was an application of the WRF model with 9 km and 1 h resolutions – in

BGD
12, 15901–15924, 2015

this case it was provided as the standard operational product of Meteodata.cz. Air temperature "T" (°C), pressure "P" (atm), U and V components of wind velocity ($\mathrm{m\,s^{-1}}$), water vapour mixing ratio "Q" (scalar) and height "h" (m), where retrieved at the two lowest levels within the atmospheric boundary layer. Over the ocean, these levels occurred roughly at 0 and 12 m heights. The standard WRF output decomposes height, temperature and pressure into their base level plus perturbation values. The WW3 wave field data for the Mediterranean was supplied by INGV using the WW3-NEMO modelling system at 0.0625° and 1 h resolutions (Clementi et al., 2013), and for the North Atlantic by Windguru at roughly 0.5° and 3 h resolutions. The variables included significant wave height "H_s" (m) and peak frequency "f_p" ($\mathrm{s^{-1}}$). The peak wave length "L_p" (m) was estimated from the peak frequency assuming the deep-water approximation: $L_p = g(1/f_p)^2/2\pi$, where g is the gravitational acceleration constant. The INGV and Windguru wave data overlapped along the Iberian shores, where they slightly mismatched the wave length and period. Therefore, the Windguru data was given a 2 : 1 ponderation relative to INGV. This procedure was sufficient to turn almost imperceptible the frontier between regions with different input data when evaluating model output (see related videos in the Results section). Sea-surface temperature (SST) and salinity (S) were estimated from the NEMO modelling system. This is the same used in the WW3-NEMO, yet provided in MyOcean catalogue comprising the whole modelled region with 1/12° and 1 day resolutions. All variables were interpolated to the same 0.09° grid (roughly 11 km at Europe's latitude) and 1 h time steps.

2.3 The model

The commonly used formula for gas exchange is given by $F = k_w(C_{air}/k_H - C_{water})$; where F represents the downward gas flux, k_H is Henry's constant (here in its C_a/C_w form) estimating the equilibrium ratio of concentrations and k_w is the transfer velocity across the infinitesimally thick water surface layer. In Wanninkhof's formulation, hence forth "Wan92", k_w ($\mathrm{cm\,h^{-1}}$) is only dependent on u_{10}: $k_w = (\alpha_{Ch} + 0.31 \cdot u_{10}^2) \cdot$

$(Sc_w/660)^{-0.5}$, where Sc_w is the Schmidt number of the water (related to viscosity), its exponent reflects the surface layer's rate of turbulent renewal, and α_{Ch} is the temperature dependent chemical enhancement due to CO_2 reaction with water given by $\alpha = 2.5 \cdot (0.5246 + 0.016256 \cdot T_w + 0.00049946 \cdot T_w^2)$. The Wind Log–Linear Profile (WLLP) was used to convert the wind velocity at height z (u_z) to the u_{10} required by Wan92. Alternatively, we tested an update to the formulation by Vieira et al. (2013) including all the processes presented below. Sc_w is determined for a given temperature and salinity following Johnson (2010). The k_w is decomposed into its wind and current drag with the bottom forcing (Eq. 1) following a principle set by Asher and Farley (1995), Borges et al. (2004), Woolf (2005), Zhang et al. (2006) and Duan and Martin (2007). However, the current drag component was not tested due to the lack of data and the still too coarse spatial resolution for this particular effect. A preliminary test disregarded k_{bubble} and estimated $k_{wind} = 1.57 \cdot 10^{-4} \cdot u_*$ following Jähne et al. (1987), hence forth "Jea87", where u_* is the friction velocity explained in the paragraph below. An alternative by Zhao et al. (2003), hence forth "ZRb03", focused on the transfer velocity dependence on wave breaking: $k_{bubble} = 0.1315 \cdot R_B^{0.6322}$, where $R_B = u_*^2/(2\pi f_p \upsilon_a)$ is the wave breaking parameter and υ_a is the kinematic viscosity of air estimated from Johnson (2010). This solution used the wave field as a proxy for the sea-surface roughness that increased transfer velocity from wind-drag with steeper younger waves (through the WLLP estimation of u_* explained below) but also as a proxy for whitecap that increased transfer velocity with wind-wave age. A more rational solution split the two drives of gas transfer (Woolf, 2005; Zhang et al., 2006): k_{wind} accounted for turbulence from wind drag keeping the Jea87 while k_{bubble} accounted for the extra turbulence and formation of bubbles from wave breaking following Zhang et al. (2006), hence forth "Zha06" (Eq. 2), where B (greek upper case Beta) is Bunsen's solubility coefficient, $W = 3.88 \times 10^{-7} R_B^{1.09}$ is the

BGD
12, 15901–15924, 2015

whitecap cover, $V = 4900$, $e = 14$ and $n = 1.2$.

$$k_\mathrm{w} = (\alpha_\mathrm{Ch} + k_\mathrm{bubble} + k_\mathrm{wind} + k_\mathrm{current}) \cdot \left(\frac{600}{\mathrm{Sc_w}}\right)^{0.5} \tag{1}$$

$$k_\mathrm{bubble} = \frac{WV}{\mathrm{B}}\left[1 + \left(e \cdot \mathrm{B} \cdot \mathrm{Sc_w}^{-1/2}\right)^{-1/n}\right]^{-n} \tag{2}$$

These formulations required the friction velocity (u_*) i.e, the speed of wind exerting drag on the sea-surface. However, wind measuring gauges are placed at a clear height from the surface – traditionally, 10 m is the reference – whereas atmospheric models estimate wind speed at fixed geopotential heights or at fixed isobaric heights. In these cases, u_* can be estimated from the Wind Log–Linear Profile (WLLP) accounting for wind speed at height z (u_z), atmospheric stability of the surface boundary layer (through ψ_m) and sea-surface roughness (through the roughness length z_0). Beware different authors give different signs to the ψ_m term besides using different notations. Here, κ is von Kármàn's constant.

$$u_* = \frac{u_z \cdot \kappa}{\ln(z) - \ln(z_0) + \psi_m(z, z_0, L)} \tag{3}$$

Roughness length is the theoretical minimal height (most often sub-milimetrical) at which average wind speed is zero. It is dependent on surface roughness and often used as its index. It is more difficult to determine over water than over land as there is a strong bidirectional interaction between wind and the surface roughness upon which wind acts. Taylor and Yelland (2001) proposed a dimensionless z_0 dependency from the wave field, increasing with the wave slope (Eq. 4a). This simple WLLP method retrieved the H_s and L_p from the WW3 data. Due to the bidirectional nature of the z_0 and u_* relation, we also tested an iterative solution where the Taylor and Yelland (2001) formulation was used as a first guess for the z_0 and the WLLP for its subsequent u_*. Afterwards, z_0 was re-estimated from the COARE 3.0 adaptation of the Taylor and Yelland (2001) formulation by adding a term for smooth flow (Eq. 4b). Then, u_* was

BGD
12, 15901–15924, 2015

re-estimated from the WLLP. Applying four iterations to the full data array were enough for an excellent convergence of this iterative WLLP method (iWLP).

$$\frac{z_0}{H_s} = 1200 \cdot \left(\frac{H_s}{L_p}\right)^{4.5} \tag{4a}$$

$$z_0 = 1200 \cdot H_s \left(\frac{H_s}{L_p}\right)^{4.5} + \frac{0.11 v_a}{u_*} \tag{4b}$$

Atmospheric stability was inferred from the vertical heat gradient as estimated by the "bulk Richardson number" ($\mathrm{Ri_b}$, Eq. 5). The algorithms by Gratchev and Fairall (1997) and Stull (1988) use the air virtual potential temperature estimated from air temperature, air pressure and specific humidity (Gratchev and Fairall, 1997) or liquid water mixing ratio (Stull, 1988). The algorithm by Lee (1997) uses the air potential temperature thus neglecting humidity. The wind velocity (u_z), temperature (T_z), pressure (P_z) and humidity (q_z) z meters above sea-surface were given by the WRF second level. The wind velocity at z_0 (u_0) was set to the theoretical $u_0 = 0$. Temperature at height 0 (T_0) was given by the SST (Grachev and Fairall, 1997; Brunke et al., 2003; Fairall et al., 2003) without rectification for cool-skin and warm-layer effects due to the lack of some required variables. Yet, these effects tend to compensate each other (Fairall et al., 1996; Zeng and Beljaars, 2005; Brunke et al., 2008). Air pressure at height 0 (P_0) was given by the WRF at the lower first level (at roughly 0 m heights). Humidity at height 0 (q_0) was set to saturation given P_0 and T_0 (Grachev and Fairall, 1997). The $\mathrm{Ri_b}$ was used to estimate the Monin–Obukhov's similarity theory length L, a discontinuous exponential function tending to $\pm\infty$ when $\mathrm{Ri_b}$ tends to ± 0 and tending to ± 0 when $\mathrm{Ri_b}$ tends to $\pm\infty$. L was used to estimate ψ_m. These were estimated either recurring to Stull's (1988) algorithm based in Businger et al. (1971) and Dyer (1974) or recurring to Lee's (1997) algorithm based in Businger et al. (1971), Dyer (1974) and Beljaars and

BGD
12, 15901–15924, 2015
Improving estimations of greenhouse gas transfer velocities
V. M. N. C. S. Vieira et al.

Holtslag (1991).

$$\mathrm{Ri_b} = \frac{g\Delta T\Delta z_i}{T\cdot u_z^2} \tag{5}$$

CO_2 is a mildly soluble greenhouse gas with a dimensionless gas-over-liquid Henry's constant of $K_{H,0} = 1.17$ for pure water at 25 °C. Its transfer velocity is limited by the molecular crossing of the water-side infinitesimally thick surface layer. Another important greenhouse gas from the carbon cycle, CH_4 is much less soluble with a $K_{H,0}$ = 31.5. In such cases the molecular crossing of the air-side infinitesimally thick surface layer should also be taken into consideration (Johnson, 2010), with the transfer velocity better estimated from the double layer "thin film" model as in Eq. (6) (Liss and Slater, 1974; Mackay and Yeun, 1983; Johnson, 2010; Vieira et al., 2013). Portraying their gas solubility determination, the relative weightings of both layers were scaled by Henry's constant dependency on water temperature, salinity, and the molecular properties of the solution (the water), the solutes (the salts) and the gas. This was tested following the numerical scheme by Sander (1999) and upgraded by Johnson (2010), or the compilation by Sarmiento and Gruber (2013) of the classical works by Weiss (1974), Weiss and Price (1980), among others. The air-side transfer velocity (k_a) was estimated from the Jeffrey et al. (2010) COARE formulation (Eq. 7), where CD is the drag coefficient and Sc_a the Schmidt number of air determined for a given temperature and salinity following Johnson (2010).

$$k = \left(\frac{1}{k_w} + \frac{k_H}{k_a}\right)^{-1} \tag{6}$$

$$k_a = \frac{u_*}{13.3\cdot \mathrm{Sc}_a^{1/2} + CD^{1/2} - 5 + \frac{\log(\mathrm{Sc}_a)}{2\kappa}} \tag{7}$$

BGD
12, 15901–15924, 2015

3 Results

From the 22 to the 26 May 2014, when the wind blew reasonably within the footprint of the Baltic atmospheric tower, the surface boundary layer was generally stable (with a few exceptions, $0 < \mathrm{Ri_b} < 0.5$) and the sea-surface was little to moderately rough ($z_0 < 0.49$ mm). Therefore, models could not be validated for a comprehensive range of conditions. Furthermore, there was wide uncertainty in the observed transfer velocities undermining elucidative estimations of the goodness-of-fits (Fig. 1). This uncertainty was largely caused by variability in the E-C estimated CO_2 fluxes, and attributable to both inherent variability of turbulent processes and measurement error. Nevertheless, comparison between model estimations clearly showed the WLLP solutions had a greater ability to adjust to local conditions. The small k_w fluctuations by Wan92 were a sole consequence of changes in water viscosity (as estimated by the $\mathrm{Sc_w}$) driven by changes in water temperature. The WLLP estimates, splitting the k_w–u_{10} data into two distinct scatter lines, the upper line corresponding to rougher sea-surfaces, demonstrated the potential of ψ_m and z_0 as additional mediators of k_w in Earth-System modelling. The iterative estimation of z_0 with the inclusion of the smooth flow (iWLP) raised k_w a little for smoother sea-surfaces. Otherwise, estimates by WLLP or iWLP overlapped.

From the 24 to the 26 May, strong winds occurred along the European shores, both on the Atlantic and on the Mediterranean. Some of these events were typical as are the cases of the storms west of Britain, the north winds along Portugal, the windy Dutch and Danish shores, the windy strait of Gibraltar, the Mistral blowing from the Alpes, the Tramontina blowing from the Pyrenees, and winter/spring storms around the Balearic islands, Sardinia, Corsica and Sicily. Besides, the air was unusually cold for the mid-spring season and colder than the sea-surface (Video 1). Consequently, the atmosphere surface boundary layer (SBL) over the seas and ocean was generally unstable (i.e, a tendency to mix), which was reflected on the properly estimated $\mathrm{Ri_b}$, L and ψ_m (Video 2). Erroneously, the $\mathrm{Ri_b}$ estimates after Lee (1997) neglecting humidity often yielded unreasonably stable SBL, besides his formulation generated complex (numbers) ψ_m whenever $L < 15z$. These problems did not occur with the $\mathrm{Ri_b}$ estimates by Gratchev and Fairall (1997) coupled to the L and ψ_m estimates by Stull (1988). Nevertheless, when both formulations were preliminarily tested with only the WRF, their estimates matched, highlighting that SBL stability over the ocean must be estimated by algorithms accounting for humidity and considering saturation at height 0. The strong winds generated plenty sea-surface agitation (Video 3). Sea-surface roughness (estimated from z_0) could be particularly high and variable along the Northeast Atlantic shoreline and inside the Mediterranean where the steeper younger waves extracted proportionally more momentum from the atmosphere (Taylor and Yelland, 2001; Fairall et al., 2003), and thus were expected to possess more turbulent surface layers through which gases were transferred at higher rates, when compared to the open-ocean under similar wind conditions. However, it must be noticed that the effect of bubble mediated transfer is not being address at the moment. The iWLP showed the smooth flow as a fundamental z_0 term, leading to significantly higher z_0 and u_* estimates than those by the WLLP (Video 4). Finally focusing on k_w, all formulations detected episodic and localized extreme events (Video 5). Relatively to the iWLP–ZRb03 conjugation, Wanninkhof's formulation overestimated k_w in the Mediterranean, whereas in the North Atlantic and North Sea the direction of the bias was highly variable. The iWLP frequently yielded higher k_w than the WLLP, highlighting the relevance of an iterative estimation of u_* and z_0. Integrated over space and time, Wanninkhof's formulation transferred 38 552 km^3 of CO_2 between atmosphere and ocean, compared to the 19 152 km^3 (49.68 %) by the iWLP–ZRb03. Their absolute differences summed to 21 518 km^3, roughly 55.82 % of the volume transferred by Wan92. Most of these situations occurred in the Mediterranean and Iberian coastal waters (Fig. 2). The inclusion of a k_a formulation in a double layer algorithm only made a pertinent difference in the CH_4 case (Video 5). When testing with N_2O, which has approximately the same solubility as CO_2, single and double layer algorithms did not made much of a difference. The fact the bias was always negative may be of lesser relevance as it may turn out

BGD
12, 15901–15924, 2015

to be only a consequence of the particular k_a and k_w formulations tested. Of greater interest is the sum of all these biases irrespective of their direction. These added to 1915 km^3 of CH_4 and 139.7 km^3 of N_2O volume when comparing single and double layer algorithms, respectively 4.97 and 0.36 % of the actual volume transferred by the single layer algorithm. This bias was proportional to the gas exchange and thus associated to windy events (Fig. 2).

4 Discussion

N_2O is a greenhouse gas 298 times more powerful than CO_2 as well as harmful to the ozone layer. Although in the open oceans it is close to equilibrium with the overlying atmosphere, the coastal oceans have consistently been observed out-gassing (Bange et al., 1996; Nevison et al., 1995, 2004; Walter et al., 2006; Barnes and Goddard, 2011; Sarmiento and Gruber, 2013). The coastal ocean is also a source of CH_4 to the atmosphere (Harley et al., 2015). Unbalanced ΔpCO_2 can occur in the open ocean associated to large gyres (Brown et al., 2015) or at the fine resolution of mesoscale eddies depending on the time the upwelled water has remained on the surface and departed its cold-core (Chen et al., 2007). But it is at the coastal ocean where the highest unbalanced atmosphere–ocean ΔpCO_2 occur, and with a fine resolution heterogeneity and intricacy of processes, associated to upwelling, plankton productivity and continental loads (Inoue et al., 2003; Rutgersson et al., 2008; Lohrenz et al., 2010; Torres et al., 2011; Oliveira et al., 2012). Consequently, there occur a significant part of the atmosphere–ocean carbon transfers (Smith and Hollibaugh, 1993; Cole and Caraco, 2001; Duarte and Prairie, 2005; Borges et al., 2005). Given the fine resolutions described above, and because Δp_{gas} and gas transfer velocities interact to yield atmosphere–ocean greenhouse gas exchanges, Earth-System modelling must represent the sea-surface with much finer space and time resolutions, and processes with much better accuracy than they currently do, particularly at the coastal ocean. Previous estimates of CO_2 uptake by the global oceans done by coarse resolution Earth-System

BGD
12, 15901–15924, 2015

modelling diverged in about 70 % depending on the transfer velocity formulations being used (Takahashi et al., 2002), whereas the wide uncertainty in the ocean N_2O source to the atmosphere mostly originated from the uncertainty in the air–water transfer velocities (Nevison et al., 1995). In our work, as the local Δp_{gas} was unknown, the estimated biases reported to volume. Nevertheless, it was demonstrated that it can be expected outstanding differences from the previously estimated atmosphere–ocean greenhouse gas exchanges. Therefore, it would not be surprising that former simulations of greenhouse gas exchange between the atmosphere and the world oceans (by Nevison et al., 1995, 2004; Walter et al., 2006; Lohrenz et al., 2010; Barnes and Goddard, 2011; Torres et al., 2011; Vichi et al., 2011; Mattia et al., 2012; Oliveira et al., 2012; Rödenbeck et al., 2013; Schuster et al., 2013; Landschützer et al., 2014; Arruda et al., 2015) would arrive at quantitatively very different results would they apply alternative formulations.

The classical approach to scale air–sea exchange parameterization is to match the global inventory of bomb-produced radiocarbon, considered the best estimator of what effectively occurred at a larger scale. Wanninkhof's formulation was calibrated with data obtained from this method. The new formulations presented in this work were remarkably consistent with Wanninkhof's formulation while also showing their benefits by representing processes with finer resolution and better accuracy (see Fig. 1). Hence, we are enthusiastic about the potential of our solution to up-scale from local to regional and global estimates. It was Wanninkhof himself suggesting his temperature dependent chemical enhancement of transfer velocity over-estimates transfer velocities at high wind speeds, and identifying the fetch dependent sea-surface agitation and atmospheric stability as neglected important factors. Simpler formulations, although trendy within the ESM community, miss-represent atmosphere–ocean gas transfer velocities, thus also miss-estimating greenhouse gas exchanges, and should be set aside giving place to more comprehensive ones. However, the later still need much improvement and validation. Our solution still needs to integrate the effects of the sea-surface cool-skin and warm-layer, surfactants and rain. But the most urgent is to improve the estimation of transfer velocity from friction velocity and wind-wave breaking, for which

BGD
12, 15901–15924, 2015

very few formulations exist, and the roughness length from the wave field. All the available formulations for these specific purposes lack robust parameter estimations. The air-side transfer velocity algorithm also needs be validated, although isolating it from the water-side transfer velocity should be a complicated task. It is a fundamental component of the double layer algorithm, required for an accurate estimation of the transfer velocity of gases with low solubility when wind blows stronger. The addition of complexity to new transfer velocity formulations must be carefully thought as these cannot become intricate to the point of calculus becoming unbearable for ESM application. In particular, any algorithm demanding an element-wise for-loop solution is unviable as it disables calculus vectorization and its coordination with parallel processing. In our software, vectorization enabled improving calculus roughly 12× faster in a single core.

The Supplement related to this article is available online at doi:10.5194/bgd-12-15901-2015-supplement.

Author contributions. V. M. N. C. S. Vieira developed the model and software, analysed the data and wrote the article; E. Sahlée provided the E-C and SAMI data; H. Pettersson provided the Directional Waverider data; P. Jurus provided the WRF data; E. Clementi provided the WW3 data; M. Mateus participated in the model and software development; all co-authors participated in the data analysis and reviewed the article.

Acknowledgements. Many thanks to Vaclav Hornik at www.windguru.cz for the data provided.

References

Artioli, Y., Blackford, J. C., Butenschön, M., Holt, J. T., Wakelin, S. L., Thomas, H., Borges, A. V., and Allen, J. I.: The carbonate system in the North Sea: sensitivity and model validation, J. Marine Syst., 102–104, 1–13, 2012.

Arruda, R., Calil, P. H. R., Bianchi, A. A., Doney, S. C., Gruber, N., Lima, I., and Turi, G.: Air–sea CO_2 fluxes and the controls on ocean surface $p$$CO_2$ variability in coastal and open-ocean southwestern Atlantic Ocean: a modeling study, Biogeosciences Discuss., 12, 7369–7409, doi:10.5194/bgd-12-7369-2015, 2015.

Asher, W. E. and Farley, P. J.: Phase-Doppler anemometer measurement of bubble concentrations in laboratory-simulated breaking waves, J. Geophys. Res., 100C, 7045–7056, 1995.

Bange, H. W., Rapsomanikis, S., and Andreae, M. O.: Nitrous oxide in coastal waters, Global Biogeochem. Cy., 10, 197–207, doi:10.1029/95GB03834, 1996.

Barnes, J. and Upstill-Goddard, R. C.: N_2O seasonal distributions and air–sea exchange in UK estuaries: implications for the tropospheric N_2O source from European coastal waters, J. Geophys. Res., 116, G01006, doi:10.1029/2009JG001156, 2011.

Beljaars, A. C. M. and Holtslag, A. A. M.: Flux parameterization over land surface for atmospheric models, J. Appl. Meteorol., 30, 327–341, 1991.

Borges, A. V., Vanderborght, J. P., Schiettecatte, L. S., Gazeau, F., Ferron-Smith, S., Delille, B., and Frankignoulle, M.: Variability of the gas transfer velocity of CO_2 in a macrotidal estuary (the Scheldt), Estuaries, 27, 593–603, 2004.

Borges, A. V., Delille, B., and Frankignoulle, M.: Budgeting sinks and sources of CO_2 in the coastal ocean: diversity of ecosystems counts, Geophys. Res. Lett., 32, L14601, doi:10.1029/2005GL023053, 2005.

Brown, P. J., Jullion, L., Landschützer, P., Bakker, D. C. E., Garabato, A. C. N., Meredith, M. P., Torres-Valdés, S., Watson, A. J., Hoppema, M., Loose, B., Jones, E. M., Telszewski, M., Jones, S. D., and Wanninkhof, R.: Carbon dynamics of the Weddell Gyre, Southern Ocean, Global Biogeochem. Cy., 29, 288–306, 2015.

Brunke, M. A, Fairall, C. W., Zeng, X., Eymard, L., and Curry, J. A.: Which bulk aerodynamic algorithms are least problematic in computing ocean surface turbulent fluxes?, J. Climate, 16, 619–635, 2003.

Brunke, M. A., Zeng, X., Misra, V., and Beljaars, A.: Integration of a prognostic sea surface skin temperature scheme into weather and climate models, J. Geophys. Res., 113, D21117, doi:10.1029/2008JD010607, 2008.

Businger, J. A., Wyngaard, J. C., Izumi, Y., and Bradley, E. F.: Flux profile relationships in the atmospheric surface layer, J. Atmos. Sci., 28, 181–189, 1971.

Carini, S., Weston, N., Hopkinson, C., Tucker, J., Giblin, A., and Vallino, J.: Gas exchange rates in the Parker River estuary, Massachusetts, Biol. Bull., 191, 333–334, 1996.

Chen, F., Cai, W.-J., Benitez-Nelson, C., and Wang, Y.: Sea surface $p\mathrm{CO_2}$–SST relationships across a cold-core cyclonic eddy: implications for understanding regional variability and air–sea gas exchange, Geophys. Res. Lett., 34, L10603, doi:10.1029/2006GL028058, 2007.

Clementi, E., Oddo, P., Korres, G., Drudi, M., and Pinardi, N.: Coupled wave–ocean modeling system in the Mediterranean Sea, Extended abstract to the 13th Int. Workshop on Wave Hindcasting, Banff, Canada, October 2013, 8 pp., 2013.

Cole, J. J. and Caraco, N. F.: Carbon in catchments: connecting terrestrial carbon losses with aquatic metabolism, Mar. Freshwater Res., 52, 101–110, 2001.

Duan, Z. and Martin, J. L.: Integration of impact factors of gas-liquid transfer rate, in: 37th Annual Mississippi Water Resources Conference, 24–25 April 2007, Jackson, MS, USA, 86–90, avialable at: http://www.wrri.msstate.edu/pdf/duan07.pdf (last access: 24 September 2015), 2007.

Dyer, A. J.: A review of flux–profile relationships, Bound.-Lay. Meteorol., 7, 363–372, 1974.

Fairall, C. W., Bradley, E. F., Godfrey, J. S., Wick, G. A., Edson, J. B., and Young, G. S.: Cool-skin and warm-layer effects on sea surface temperature, J. Geophys. Res., 101, 1295–1308, 1996.

Fairall, C. W., Bradley, E. F., Hare, J. E., Grachev, A. A., and Edson, J. B.: Bulk parameterization of air–sea fluxes: updates and verification for the COARE algorithm, J. Climate, 16, 571–591, 2003.

Fogli, P. G., Manzini, E., Vichi, M., Alessandri, A., Patara, L., Gualdi, S., Scoccimarro, E., Masina, S., and Navarra, A.: INGV-CMCC Carbon (ICC): a Carbon Cycle Earth System Model, Technical Report 61, Centro Euro–Mediterraneo per I Cambiamenti Climatici, ANS Division, Bologna, Italy, 2009.

Gangstø, R., Joos, F., and Gehlen, M.: Sensitivity of pelagic calcification to ocean acidification, Biogeosciences, 8, 433–458, doi:10.5194/bg-8-433-2011, 2011.

Gattuso, J.-P., Frankignoulle, M., and Wollast, R.: Carbon and carbonate metabolism in coastal aquatic ecosystems, AnnU. Rev. Ecol. Syst., 29, 405–434, 1998.

Grachev, A. A. and Fairall, C. W.: Dependence of the Monin–Obukhov Stability Parameter on the bulk Richardson Number over the ocean, J. Appl. Meteorol., 36, 406–414, 1997.

Harley, J. F., Carvalho, L., Dudley, B., Heal, K. V., Rees, R. M., and Skiba, U.: Spatial and seasonal fluxes of the greenhouse gases N_2O, CO_2 and CH_4 in a UK macrotidal estuary, Estuar. Coast. Shelf S., 153, 62–73, 2015

Inoue, H. Y., Ishii, M., Matsueda, H., Kawano, T., Murata, A., and Takasugi, Y.: Distribution of the partial pressure of CO_2 in surface water (pCO_2^w) between Japan and the Hawaiian Islands: pCO_2^w–SST relationship in the winter and summer, Tellus B, 55, 456–465, 2003.
Jähne, B., Munnich, K. O., Bosinger, R., Dutzi, A., Huber, W., and Libner, P.: On the parameters influencing air–water gas exchange, J. Geophys. Res., 92, 1937–1949, 1987.
Jeffery, C., Robinson, I., and Woolf, D.: Tuning a physically-based model of the air–sea gas transfer velocity, Ocean Model., 31, 28–35, doi:10.1016/j.ocemod.2009.09.001, 2010.
Johnson, M. T.: A numerical scheme to calculate temperature and salinity dependent air–water transfer velocities for any gas, Ocean Sci., 6, 913–932, doi:10.5194/os-6-913-2010, 2010.
Landschützer, P., Gruber, N., Bakker, D. C. E., and Schuster, U.: Recent variability of the global ocean carbon sink, Global Biogeochem. Cy., 28, 927–949, 2014.
Lazzari, P., Solidoro, C., Ibello, V., Salon, S., Teruzzi, A., Béranger, K., Colella, S., and Crise, A.: Seasonal and inter-annual variability of plankton chlorophyll and primary production in the Mediterranean Sea: a modelling approach, Biogeosciences, 9, 217–233, doi:10.5194/bg-9-217-2012, 2012.
Lee, H. N.: Improvement of surface flux calculations in the atmospheric surface layer, J. Appl. Meteorol., 36, 1416–1423, 1997.
Lohrenz, S. E., Cai, W. J., Chen, F., Chen, X., and Tuel, M.: Seasonal variability in air–sea fluxes of CO_2 in a river-influenced coastal margin, J. Geophys. Res.-Oceans, 115, C10034, doi:10.1029/2009JC005608, 2010.
Mattia, G., Vichi, M., Zavatarelli, M., and Oddo, P.: The wind-driven response of the Mediterranean sea biogeochemistry to the Eastern Mediterranean Transient. A numerical model study, Geophysical Research Abstracts, EGU General Assembly 2012, held 22–27 April, 2012 in Vienna, Austria, 4437 pp., 14, EGU2012-4437, 2012.
Muller-Karger, F. E., Varela, R., Thunell, R., Luerssen, R., Hu, C., and Walsh, J. J.: The importance of continental margins in the global carbon cycle, Geophys. Res. Lett., 32, doi:10.1029/2004GL021346, 2005.
Nevison, C. D., Weiss, R. F., and Erickson III, D. J.: Global oceanic emissions of nitrous oxide, J. Geophys. Res., 100, 15809–15820, 1995.
Nevison, C. D., Lueker, T. J., and Weiss, R. F.: Quantifying the nitrous oxide source from coastal upwelling, Global Biogeochem. Cy., 18, GB1018, doi:10.1029/2003GB002110, 2004.
OCMIP: Ocean Carbon-Cycle Model Intercomparison Project, available at: http://ocmip5.ipsl.jussieu.fr/OCMIP, last updated: 2004 (last access: 27 August 2015), 2004.

BGD
12, 15901–15924, 2015

Oliveira, A. P., Cabeçadas, G., and Pilar-Fonseca, T.: Iberia coastal ocean in the CO_2 sink/source context: Portugal case study, J. Coastal Res., 28, 184–195, 2012.

Raymond, P. A. and Cole, J. J.: Gas exchange in rivers and estuaries choosing a gas transfer velocity, Estuaries, 24, 312–317, 2001.

Rödenbeck, C., Keeling, R. F., Bakker, D. C. E., Metzl, N., Olsen, A., Sabine, C., and Heimann, M.: Global surface-ocean p^{CO_2} and sea–air CO_2 flux variability from an observation-driven ocean mixed-layer scheme, Ocean Sci., 9, 193–216, doi:10.5194/os-9-193-2013, 2013.

Rutgersson, A., Norman, M., Schneider, B., Petterson, H., and Sahlée, E.: The annual cycle of carbon dioxide and parameters influencing the air–sea carbon exchange in the Baltic Proper, J. Marine Syst., 74, 381–394, 2008.

Sander, R.: Compilation of Henry's Law Constants for Inorganic and Organic Species of Potential Importance in Environmental Chemistry (Version 3), available at: http://www.henrys-law.org (last access: 24 September 2015), 1999.

Sarmiento, J. L. and Gruber, N.: Ocean Biogeochemical Dynamics, Princeton University Press, New Jersey, USA, 528 pp., 2013.

Schuster, U., McKinley, G. A., Bates, N., Chevallier, F., Doney, S. C., Fay, A. R., González-Dávila, M., Gruber, N., Jones, S., Krijnen, J., Landschützer, P., Lefèvre, N., Manizza, M., Mathis, J., Metzl, N., Olsen, A., Rios, A. F., Rödenbeck, C., Santana-Casiano, J. M., Takahashi, T., Wanninkhof, R., and Watson, A. J.: An assessment of the Atlantic and Arctic sea–air CO_2 fluxes, 1990–2009, Biogeosciences, 10, 607–627, doi:10.5194/bg-10-607-2013, 2013.

Smith, S. V. and Hollibaugh, J. T.: Coastal metabolism and the oceanic organic carbon balance, Rev. Geophys., 31, 75–89, 1993.

Takahashi, T., Sutherland, S. C., Sweeney, C., Poisson, A., Metzl, N., Tilbrook, B., Bates, N., Wanninkhof, R., Feelyf, R. A., Sabine, C., Olafsson, J., and Nojirih, Y.: Global sea–air CO_2 flux based on climatological surface ocean pCO_2, and seasonal biological and temperature effects, Deep-Sea Res., 49, 1601–1622, 2002.

Takahashi, T., Sutherland, S. C., Wanninkhof, R., Sweeney, C., Feely, R. A., Chipman, D. W., Hales, B., Friederich, G., Chavez, F., Watson, A., Bakker, D. C. E., Schuster, U., Metzl, N., Yoshikawa-Inoue, H., Ishii, M., Midorikawa, T., Nojiri, Y., Sabine, C., Olafsson, J., Arnarson, T. S., Tilbrook, B., Johannessen, T., Olsen, A., Bellerby, R., Körtzinger, A., Steinhoff, T., Hoppema, M., de Baar, H. J. W., Wong, C. S., Delille, B., and Bates, N. R.: Climatological mean and decadal changes in surface ocean pCO_2, and net sea–air CO_2 flux over the global oceans, Deep-Sea Res. Pt. II, 56, 554–577, 2009.

Taylor, P. K. and Yelland, M. J.: The dependence of sea surface roughness on the height and steepness of the waves, J. Phys. Oceanogr., 31, 572–590, 2001.

Torres, R., Pantoja, S., Harada, N., González, H. E., Daneri, G., Frangopulos, M., Rutllant, J. A., Duarte, C. M., Rúiz-Halpern, S., Mayol, E., and Fukasawa, M.: Air–sea CO_2 fluxes along the coast of Chile: from CO_2 outgassing in central northern upwelling waters to CO_2 uptake in southern Patagonian fjords, J. Geophys. Res., 116, C09006, doi:10.1029/2010JC006344, 2011.

Vichi, M., Masina, S., and Navarra, A.: A generalized model of pelagic biogeochemistry for the global ocean ecosystem. Part II: Numerical simulations, J. Marine Syst., 64, 110–134, doi:10.1016/j.jmarsys.2006.03.014, 2007a.

Vichi, M., Pinardi, N., and Masina, S.: A generalized model of pelagic biogeochemistry for the global ocean ecosystem. Part I: Theory, J. Marine Syst., 64, 89–109, doi:10.1016/j.jmarsys.2006.03.006, 2007b.

Vichi, M., Manzini, E., Fogli, P. G., Alessandri, A. Patara, L., Scoccimarro, E., Masina, S., and Navarra, A.: Global and regional ocean carbon uptake and climate change: sensitivity to an aggressive mitigation scenario, Clim. Dynam., 37, 1929–1947, 2011.

Vieira, V. M. N. C. S., Martins, F., Silva, J., and Santos, R.: Numerical tools to estimate the flux of a gas across the air–water interface and assess the heterogeneity of its forcing functions, Ocean Sci., 9, 355–375, doi:10.5194/os-9-355-2013, 2013.

Visinelli, L., Masina, S., Vichi, M., and Storto, A.: Impacts of physical data assimilation on the Global Ocean Carbonate System, Biogeosciences Discuss., 11, 5399–5441, doi:10.5194/bgd-11-5399-2014, 2014.

Walter, S., Bange, H. W., Breitenbach, U., and Wallace, D. W. R.: Nitrous oxide in the North Atlantic Ocean, Biogeosciences, 3, 607–619, doi:10.5194/bg-3-607-2006, 2006.

Wanninkhof, R.: Relationship between wind speed and gas exchange over the ocean, J. Geophys. Res., 97, 7373–7382, 1992.

Webb, E. K., Pearman, G. I., and Leuning, R.: Correction of flux measurements for density effects due to heat and water vapour transfer, Q. J. Roy. Meteor. Soc., 106, 85–100, 1980.

Weiss, R. F.: Carbon dioxide in water and seawater: the solubility ofa non-ideal gas, Mar. Chem., 2, 203–215, 1974.

BGD
12, 15901–15924, 2015

Improving estimations of greenhouse gas transfer velocities

V. M. N. C. S. Vieira et al.

Weiss, R. F. and Price, B. A.: Nitrous oxide solubility in water and seawater, Mar. Chem., 8, 347–359, 1980.

Woolf, D. K.: Parameterization of gas transfer velocities and seastate-dependent wave breaking, Tellus B, 57, 87–94, 2005.

Zeng, X. and Beljaars, A.: A prognostic scheme of sea surface skin temperature for modeling and data assimilation, Geophys. Res. Lett., 32, L14605, doi:10.1029/2005GL023030, 2005.

Zhang, W., Perrie, W., and Vagle, S.: Impacts of winter storms on air–sea gas exchange, Geophys. Res. Lett., 33, L14803, doi:10.1029/2005GL025257, 2006.

Zhao, D., Toba, Y., Suzuki, Y., and Komori, S.: Effect of wind waves on air–sea gas exchange: proposal of an overall CO_2 transfer velocity formula as a function of breaking-wave parameter, Tellus B, 55, 478–487, 2003.

BGD

12, 15901–15924, 2015

Improving estimations of greenhouse gas transfer velocities

V. M. N. C. S. Vieira et al.

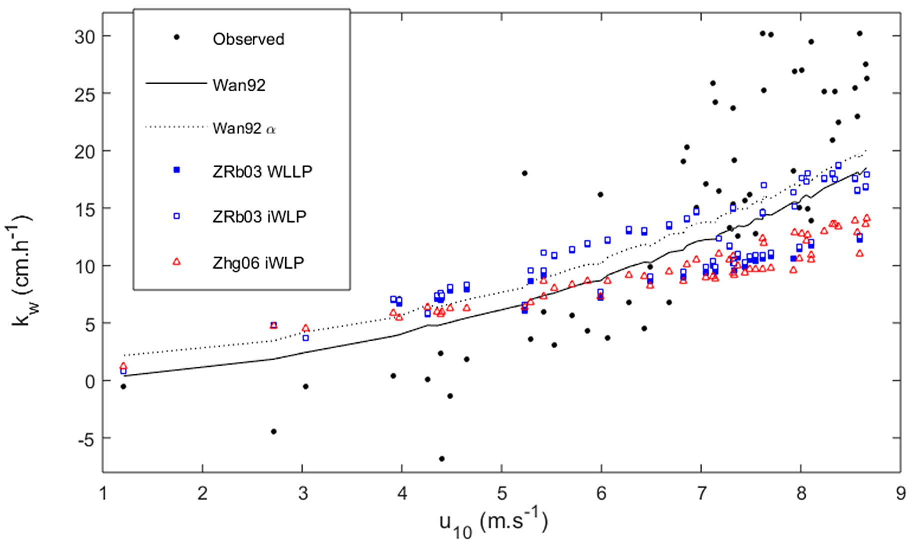

Figure 1. Model validation with the Baltic Sea data.

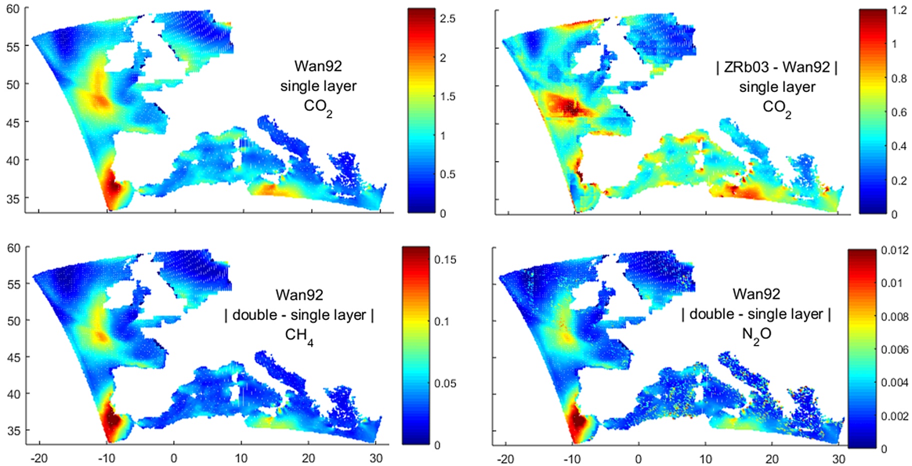

Figure 2. Gas volume exchanged over the tested time interval: (upper left) as forecasted by Wan92, (upper right) absolute difference between CO_2 exchanged by Wan92 and by the iWLP–ZRb03 conjugation, and (bottom left and bottom right) absolute differences of (bottom left) CH_4 and (bottom right) N_2O exchanged by single or double layer algorithms. Colorscale: $km^3\ 66\,h^{-1}$.

BGD
12, 15901–15924, 2015

Improving estimations of greenhouse gas transfer velocities

V. M. N. C. S. Vieira et al.